

# Effects of Superheating on Thermodynamic Performance of Organic Rankine Cycles

Kyoung Hoon Kim

**Abstract**—Recently ORC(Organic Rankine Cycle) has attracted much attention due to its potential in reducing consumption of fossil fuels and its favorable characteristics to exploit low-grade heat sources. In this work thermodynamic performance of ORC with superheating of vapor is comparatively assessed for various working fluids. Special attention is paid to the effects of system parameters such as the evaporating temperature and the turbine inlet temperature on the characteristics of the system such as maximum possible work extraction from the given source, volumetric flow rate per 1 kW of net work and quality of the working fluid at turbine exit as well as thermal and exergy efficiencies. Results show that for a given source the thermal efficiency increases with decrease of the superheating but exergy efficiency may have a maximum value with respect to the superheating of the working fluid. Results also show that in selection of working fluid it is required to consider various criteria of performance characteristics as well as thermal efficiency.

**Keywords**—organic Rankine cycle (ORC), low-grade energy source, Patel-Teja equation, thermodynamic performance

## I. INTRODUCTION

THE amount of waste heat from eleven industrial complexes in Korea was detected 148,913 TOE/year, and it was analyzed that 83% of the waste heat was in the temperature range from 0°C to 200°C, so low-grade energy. It was also evaluated that 82% of the waste heat was exhausted by flue gas, so in the form of sensible energy [1]. Statistical investigations indicate that low-grade waste heat accounts for 50% or more of the total heat generated in industry. Due to lack of efficient recovery methods, low-grade waste heat has generally been discarded in industry. Typical low-grade heat sources are waste heat from industry, geothermal heat, and solar energy. Therefore, more and more attention has been paid to the utilization of low-grade heat nowadays for its potential in reducing fossil fuel consumption and alleviating environmental problems [2].

In recent years, organic Rankine cycle has become a field of intense research and appears as a promising technology for conversion of heat into useful work of electricity. In an ORC the saturation vapor curve is the most crucial characteristics of a working fluid. This characteristic affects the fluid applicability, cycle efficiency, and arrangement of associated equipment in a power generation system. There are generally three types of vapor saturation curves in the temperature-entropy diagram: a dry fluid with positive slope of  $dT/dS$ , a wet fluid with negative slope of  $dT/dS$ , and an isentropic fluid with nearly infinitely large slopes [3]. Drescher and Brüggemann [4] investigate the

ORC in solid biomass power and heat plants. They propose a method to find suitable thermodynamic fluids for ORCs in biomass plants and found that the family of alkylbenzenes showed the highest efficiency.

Dai et al. [5] use a generic optimization algorithm, identified isobutane and R236ea as efficient working fluids. Hung et al. [6] examine Rankine cycles using organic fluids which are categorized into three groups of wet, dry and isentropic fluids. They point out that dry fluids have disadvantages of reduction of net work due to superheated vapor at turbine exit, and wet fluids of the moisture content at turbine inlet, so isentropic fluids are to be preferred. Heberle and Brüggemann [7] investigate the combined heat and power generation for geothermal resources with series and parallel circuits of an ORC. Tranche et al. [8] investigate comparatively the performance of solar organic Rankine cycle using various working fluids. Volume flow rate, mass flow rate, power ratio as well as thermal efficiency are used for comparison.

In this paper, the thermodynamic performance of ORC with superheater is comparatively investigated for various working fluids including wet, dry and isentropic fluids. The various thermodynamic characteristics of the ORC such as pressure ratio, specific power and volume flow rate as well as thermal efficiency or exergy efficiency are investigated in terms of the parameters such as evaporating temperature and turbine inlet temperature. And special attention is focus on the maximum extraction of useful work generation from the given energy source.

## II. SYSTEM ANALYSIS

The working fluids considered in this work are nine fluids of  $\text{NH}_3$ , R123, R134a, R143a, R152a,  $\text{iC}_4\text{H}_{10}$ ,  $\text{iC}_5\text{H}_{12}$ ,  $\text{C}_6\text{H}_6$ , and  $\text{C}_8\text{H}_{10}$ . In this work the thermodynamic properties of the working fluids are calculated by Patel-Teja equation of state [9-10]. The basic data of the fluids which are needed to calculate Patel-Teja equation are shown in TABLE 1, where  $M$ ,  $T_c$ ,  $P_c$  and  $\omega$  are molecular weight, critical temperature, critical pressure, and accentric factor, respectively [11]. The molecular weights of  $\text{NH}_3$  and  $\text{iC}_4\text{H}_{10}$  are small, and those of R123 and  $\text{C}_8\text{H}_{12}$  are large among the fluids. The critical temperatures of R143a and R134a are low and those of  $\text{C}_8\text{H}_{10}$  and  $\text{C}_6\text{H}_6$  are high. The critical pressures of  $\text{iC}_5\text{H}_{12}$  and  $\text{C}_8\text{H}_{10}$  are low and those of  $\text{NH}_3$  and  $\text{C}_6\text{H}_6$  are high. The temperature-entropy diagrams for the fluids are shown in Fig. 1. It can be seen from the figure that R123,  $\text{iC}_4\text{H}_{10}$ ,  $\text{iC}_5\text{H}_{12}$ ,  $\text{C}_6\text{H}_6$ , and  $\text{C}_8\text{H}_{10}$  belong to dry fluids, R134a and R143a to isentropic fluids, and  $\text{NH}_3$  and R152a to

K. H. Kim is with Department of Mechanical Engineering, Kumoh National Institute of Technology, 1 Yangho, Gumi, Gyeongbuk 730-701, Korea (phone: 82-54-478-7292; fax: 82-54-478-7319; e-mail: khkim@kumoh.ac.kr).

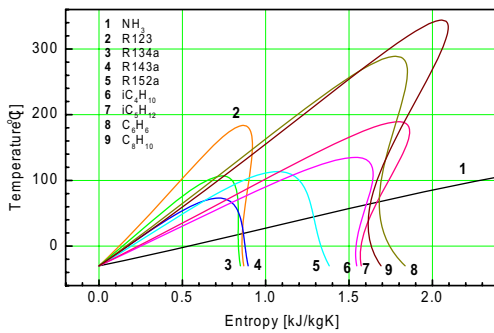


Fig. 1 Temperature-entropy diagrams for the working fluids

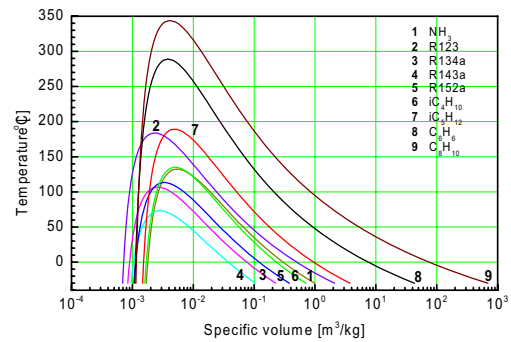
wet fluids. Especially, latent heat of vaporization of  $\text{NH}_3$  is much greater than the others so the whole temperature-entropy diagram for  $\text{NH}_3$  is not shown in the figure. The temperature-volume diagrams of the fluids are shown in Fig.2. The volume of saturated vapor at a given temperature is large for  $\text{C}_8\text{H}_{10}$  or  $\text{C}_6\text{H}_6$ , and small for R143a or R134a.

The schematic diagram of the system is shown in Fig. 3. The system consists of a preheater, an evaporator, superheater, a turbine, a condenser, and a pump. A low-grade energy is supplied to the system as sensible heat energy at point s0 and exhausted at s3.

Important assumptions used in this work are as follows.

- 1) The energy source is air at temperature of  $T_s$ .
- 2) The working fluid leaves the condenser as saturated liquid at temperature of  $T_L$ .
- 3) The evaporating temperature,  $T_E$  is lower than the critical temperature of the fluid and the turbine inlet temperature becomes  $T_s - \Delta T_H$  by the superheater.
- 4) The mass flow rate of the working fluid is operated at the maximum value in order to generate the maximum useful work from a given source of energy.
- 5) Pressure drop and heat loss of the systems are negligible.

At point 1, the fluid is saturated liquid at  $T_L$  and the corresponding saturated pressure  $P_L$  is the condensing pressure of the system. When the evaporating temperature is  $T_E$ , the thermodynamic properties at points 3 and 4 are determined as the saturated liquid and vapor at  $T_E$ , respectively and the corresponding saturation pressure  $P_H$  is the evaporating pressure of the system. The thermodynamic properties at point 4 are determined with temperature  $T_H$  and pressure  $P_H$ . The thermody-



amic properties at points 2 and 6 are determined with the isentropic efficiencies of pump and turbine,  $\eta_p$  and  $\eta_t$ , respectively. Then heat addition and net work per unit mass of a working fluid  $q_{in}$  and  $w_{net}$ , and thermal efficiency  $\eta_{th}$  are obtained as

$$q_{in} = h_5 - h_2 \quad (1)$$

$$w_{net} = w_t - w_p = (h_5 - h_6) - (h_2 - h_1) \quad (2)$$

$$\eta_{th} = w_{net} / q_{in} \quad (3)$$

where  $h$  denotes specific enthalpy and subscripts  $t$  and  $p$  denote turbine and pump, respectively. As the mass flow rate of working fluid for a given energy source increases, the temperature of source flow at evaporator exit decreases, and finally the temperature difference between the source and the working fluid reaches the pinch point,  $\Delta T_{PP}$  when the mass flow rate of working fluid is increased to its maximum value. Then the ratio of mass flow rate of a working fluid to that of the source,  $r_m$ , can be determined as

$$r_m = \frac{\dot{m}_{wf}}{\dot{m}_s} = \frac{c_{ps}(T_{s0} - T_{s3})}{h_5 - h_3} \quad (4)$$

$$T_{s3} = T_s + \Delta T_{PP} \quad (5)$$

where subscripts  $wf$  or  $s$  denotes the working fluid or the source, respectively, and  $\dot{m}$  the mass flow rate, and  $\Delta T_{PP}$  the pinch point of the exchangers.

In this work enthalpy ratio,  $x$ , is defined as

substance	M (kg/kmol)	Tc (K)	Pc (bar)	$\omega$
$\text{NH}_3$	17.031	405.65	112.78	0.252
R123	136.467	456.90	36.74	0.282
R134a	102.031	380.00	36.90	0.239
R143a	84.041	346.25	37.58	0.253
R152a	66.051	386.60	44.99	0.263
$i\text{C}_4\text{H}_{10}$	58.123	408.14	36.48	0.177
$i\text{C}_5\text{H}_{12}$	72.150	462.43	33.81	0.228
$\text{C}_6\text{H}_6$	78.114	562.16	48.98	0.211
$\text{C}_8\text{H}_{10}$	106.167	617.17	36.09	0.304

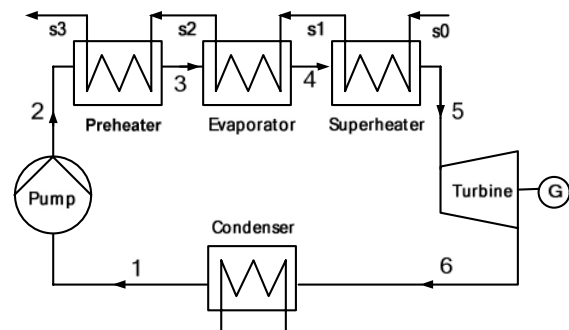


Fig. 3 Schematic diagram of the system

TABLE II  
BASIC CALCULATION CONDITIONS

symbol	Parameter	data	unit
$T_S$	source temperature	200	$^{\circ}\text{C}$
$T_L$	condensing temperature	20	$^{\circ}\text{C}$
$\Delta T_H$	temperature difference at source inlet	15	$^{\circ}\text{C}$
$\Delta T_{PP}$	pinch point	5	$^{\circ}\text{C}$
$\eta_p$	isentropic efficiency of pump	0.80	
$\eta_t$	isentropic efficiency of turbine	0.80	
	source	air	

$$x = \frac{h - h_f}{h_g - h_f} \quad (6)$$

where  $h_f$  or  $h_g$  denotes specific enthalpy of saturated liquid or vapor of the working fluid, respectively. So when  $0 \leq x \leq 1$ ,  $x$  is same as the quality of the fluid and the fluid is the mixture of saturated liquid and vapor. When  $x < 0$ , the fluid is a compressed liquid, and when  $x > 1$ , the fluid is a superheated vapor.

### III. RESULTS AND DISCUSSIONS

The system parameters used in this work are summarized in Table II. In this work the basic data for analysis are  $T_S = 200^{\circ}\text{C}$  and  $\Delta T_H = 15^{\circ}\text{C}$ , so the turbine inlet temperature in this work is fixed at  $T_H = T_S - \Delta T_H = 185^{\circ}\text{C}$ . Fig. 4 shows effects of the evaporating temperature on the enthalpy ratio for various working fluids. It can be seen from the figure that the enthalpy ratio increases as the evaporating temperature decreases, namely, the superheating of the vapor increases. Enthalpy ratio of R143a or  $i\text{C}_4\text{H}_{10}$  is relatively high, and that of  $\text{NH}_3$  or  $\text{C}_6\text{H}_6$  is relatively low. And it can be also seen that for even wet fluids like  $\text{NH}_3$  the enthalpy ratio at the exit of turbine can be greater than one or a certain limit value so the wet fluids should not be pre-excluded during the selection process of proper working fluids. On the other hand, as this work is limited to the case that the evaporating temperature is lower than the critical temperature of the fluid, i.e., the phase transition from liquid of vapor exists, the working fluid whose critical temperature is low such as R143a, R152a, R134a, or  $\text{NH}_3$  does not show its data for  $T_E > T_c$ .

Fig. 5 shows effects of the evaporating temperature on the net work per unit mass of fluid for various working fluids. The figure shows that the net work per unit mass of fluid generally increases as the evaporating temperature decreases, namely, the

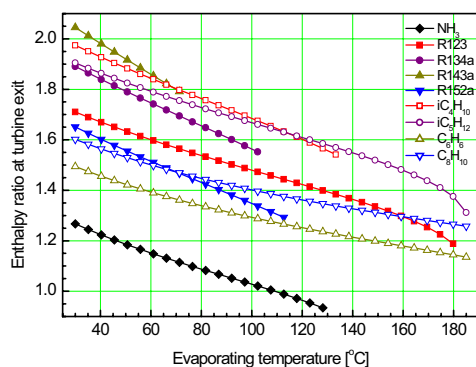


Fig. 4 Enthalpy ratio at turbine exit as a function of the evaporating temperature for various working fluids

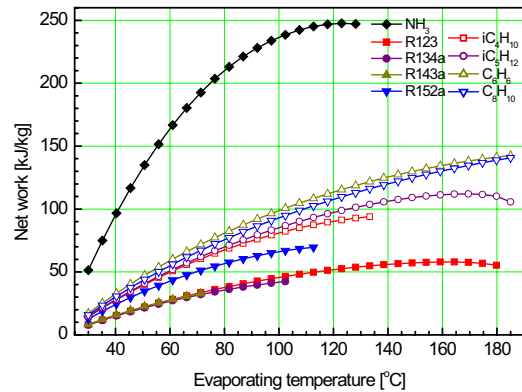


Fig. 5 Net work per unit mass of working fluid as a function of the evaporating temperature for various working fluids

superheating of the vapor increases. Net work of  $\text{NH}_3$  is much higher than those of other fluids, and net work of  $\text{C}_6\text{H}_6$  or  $\text{C}_8\text{H}_{10}$  is relatively high, and R143a or R134a is relatively low. In the case  $i\text{C}_5\text{H}_{12}$  or R123, there exists an optimal value of the net work with respect to the evaporating temperature.

Fig. 6 shows effects of the evaporating temperature on the thermal efficiency for various working fluids. The figure shows that the thermal efficiency increases as the evaporating temperature decreases, namely, the superheating of the vapor increases. Thermal efficiency of  $\text{C}_6\text{H}_6$ ,  $\text{C}_8\text{H}_{10}$  or  $\text{NH}_3$  is relatively high, whereas  $i\text{C}_4\text{H}_{10}$  or  $i\text{C}_5\text{H}_{12}$  is relatively low.

Fig. 7 shows effects of the evaporating temperature on the ratio of mass flow rate of working fluid to that of source to generate maximum power from the given energy source. The figure shows diverse behaviors of the ratio with respect to the evaporating temperature. As the evaporating temperature increases, the ratio of R143a increases, the ratio of  $\text{NH}_3$  remains nearly constant, the ratios of R123,  $i\text{C}_5\text{H}_{12}$ ,  $\text{C}_8\text{H}_{10}$ , and  $\text{C}_6\text{H}_6$  decrease, and each of the ratios of R134a, R152a, and  $i\text{C}_4\text{H}_{10}$  has its minimum value. The ratios of R143a, R134a, and R123 are relatively high, whereas the ratios of  $\text{C}_6\text{H}_6$ ,  $\text{C}_8\text{H}_{10}$  and  $\text{NH}_3$  are relatively low. Fig. 8 shows effects of the evaporating temperature on the net work per unit mass of the given energy

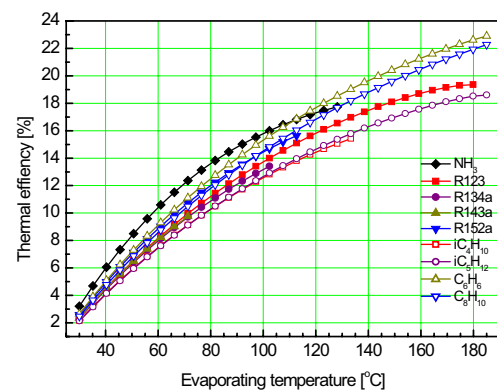


Fig. 6 Thermal efficiency as a function of the evaporating temperature for various working fluids

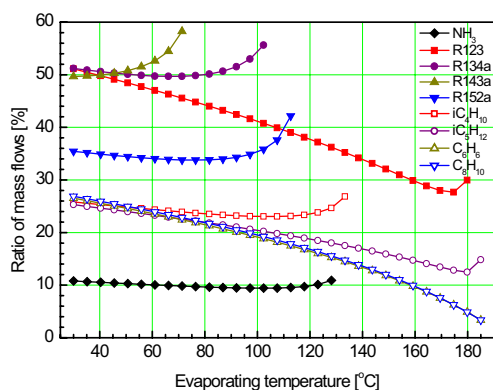


Fig. 7 Ratio of mass flow rate of working fluid to that of source as a function of the evaporating temperature

source for various working fluids. The figure shows that the net works of  $\text{NH}_3$ , R152a, R143a,  $\text{iC}_4\text{H}_{10}$  increase, however, each of the net works of R123,  $\text{iC}_5\text{H}_{12}$ ,  $\text{C}_8\text{H}_{10}$ , and  $\text{C}_6\text{H}_6$  increases first and reaches its maximum value and subsequently decreases so it has an optimal value. Fig. 9 shows effects of the evaporating temperature on the volume flow rate at the turbine exit to produce 1 kW of net work for various working fluids. It can be seen from the figure that the volume flow rate of a working fluid to produce the same amount of net work is small for  $\text{NH}_3$  or R143a and large for  $\text{C}_8\text{H}_{10}$  or  $\text{C}_6\text{H}_6$ . Since the volume flow rate to produce a same amount of net work relates directly with the size and cost of the turbine,  $\text{C}_8\text{H}_{10}$  or  $\text{C}_6\text{H}_6$  is not a proper working fluid for the system because of its too large volume flow rate. This fact means that various thermodynamic properties such as volume flow rate per 1 kW net work as well as thermal efficiency should be tested for the selection of a proper working fluid.

#### IV. CONCLUSIONS

In this paper, the performance of organic Rankine cycle with superheating has been thermodynamically analyzed. The main results are as follows.

- For a fixed source temperature, the net work per unit mass of working fluid increases, as superheating of vapor increases, i.e., evaporating temperature decreases. However, the maximum network per unit mass of source has an optimal value with respect to the evaporating temperature.
- The volume flow rate per 1 kW of net work would be a good criterion for selection of working fluid. The volume flow rate of  $\text{C}_8\text{H}_{10}$  or  $\text{C}_6\text{H}_6$  is much higher than that of others.
- There is no working fluid which is the best for every aspect of thermodynamic performance. So for the selection of a working fluid, various thermodynamic properties should be synthetically and comparatively considered.

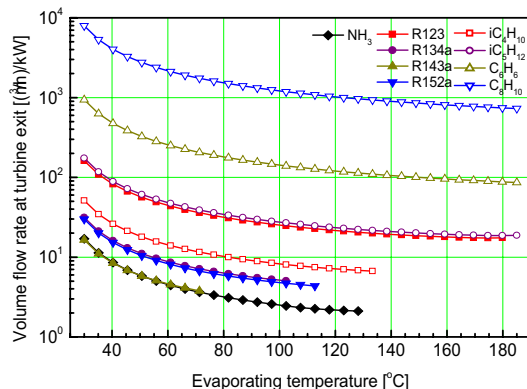


Fig. 9 Volume flow rate of working fluid at turbine exit to produce 1 kW of electricity as a function of the evaporating temperature

#### ACKNOWLEDGMENT

This research was supported by Basic Science Research Program through the National Research Foundation of Korea (NRF) funded by the Ministry of Education, Science and Technology (No. 2010-0007355).

#### REFERENCES

- [1] Y.C. Choi, T.J. Park, J.C. Hong, S.Y. Cho, A study on the characteristics of waste heat from the industrial complexes for residential and commercial sectors, *Energy Eng. J.* 8(1999) 242-247(Korean).
- [2] N.A. Lai, M. Wendland, J. Fisher, Working fluids for high temperature organic Rankine cycle, *Energy* 36(2011) 199-211.
- [3] T.C. Hung, T.Y. Shai, S.K. Wang, A review of organic Rankine cycles (ORCs) for the recovery of low-grade waste heat, *Energy* 22(1997) 661-667.
- [4] U. Drescher, D. Brueggemann, Fluid selection for the organic Rankine cycle (ORC) in biomass power and heat plants, *Applied Thermal Eng.* 27(2007) 223-228.
- [5] Y. Dai, J. Wang, L. Gao, Parametric optimization and comparative study of organic Rankine cycle (ORC) for low grade waste heat recovery, *Energy Conv. Mgmt.* 50(2009) 576-582.
- [6] T.C. Hung, S.K. Wang, C.H. Kuo, B.S. Pei, K.F. Tsai, A study of organic working fluids on system efficiency of an ORC using low-grade energy sources, *Energy* 35(2010) 1403-1411.
- [7] F. Heberle, D. Brueggemann, Exergy based fluid selection for a geothermal organic Rankine cycle for combined heat and power generation, *Applied Thermal Eng.* 30(2010) 1326-1332.
- [8] Tchanché B.F, Papadakis G, Frangoudakis A : "Fluid selection for a low-temperature solar organic Rankine cycle," *Applied Thermal Eng.*, Vol. 29, 2009, pp. 2468-2476.
- [9] T. Yang, G.J. Chen, T.M. Guo, Extension of the Wong- Sandler mixing rule to the three-parameter Patel-Teja equation of state: Application up to the near-critical region, *Chem. Eng. J.* 67(1997) 27-36.
- [10] J. Gao, L.D. Li, Z.Y. Zhu, S.G. Ru S.G, Vapor-liquid equilibria calculation for asymmetric systems using Patel-Teja equation of state with a new mixing rule, *Fluid Phase Equilibria* 224(2004) 213- 219.
- [11] C.L. Yaws, *Chemical properties handbook*, McGraw- Hill (1999).